



ELSEVIER

Contents lists available at SciVerse ScienceDirect

Talanta

journal homepage: [www.elsevier.com/locate/talanta](http://www.elsevier.com/locate/talanta)

# HPLC/ELSD analysis of amidated bile acids: An effective and rapid way to assist continuous flow chemistry processes

Roccardo Sardella, Antimo Gioiello, Federica Ianni, Francesco Venturoni, Benedetto Natalini\*

Dipartimento di Chimica e Tecnologia del Farmaco, Università degli Studi di Perugia, Perugia, Italy

## ARTICLE INFO

### Article history:

Received 11 May 2012

Received in revised form

26 July 2012

Accepted 31 July 2012

Available online 10 August 2012

### Keywords:

*N*-Acyl amidation

Glyco-bile acids

Tauro-bile acids

Continuous flow synthesis

Method validation

Evaporative light scattering detector

## ABSTRACT

The employment of the flow *N*-acyl amidation of natural bile acids (BAs) required the *in-line* connection with suitable analytical tools enabling the determination of reaction yields as well as of the purity grade of the synthesized glyco- and tauro-conjugated derivatives. In this framework, a unique HPLC method was successfully established and validated for ursodeoxycholic (UDCA), chenodeoxycholic (CDCA), deoxycholic (DCA) and cholic (CA) acids, as well as the corresponding glyco- and tauro-conjugated forms. Because of the shared absence of relevant chromophoric moieties in the sample structure, an evaporative light scattering detector (ELSD) was profitably utilized for the analysis of such steroidal species. For each of the investigated compounds, all the runs were contemporarily carried out on the acidic free and the two relative conjugated variants. The different ELSD response of the free and the corresponding conjugated BAs, imposed to build-up separate calibration curves. In all the cases, very good precision (RSD% values ranging from 1.04 to 6.40% in the long-period) and accuracy (Recovery% values ranging from 96.03 to 111.14% in the long-period) values along with appreciably low LOD and LOQ values (the former being within the range 1–27 ng mL<sup>-1</sup> and the latter within the range 2–44 ng mL<sup>-1</sup>) turned out.

© 2012 Elsevier B.V. All rights reserved.

## 1. Introduction

Bile acids (BAs) are the catabolic product of hepatic cholesterol and represent the principal active components of bile. Placed at the interface between nutrient absorption and metabolism, they act as natural detergents that, when released into the intestine following a meal, facilitate the absorption of dietary lipids and fat-soluble nutrients [1–3]. A number of recent evidences have led to a profound revolution in the BA research, being now considered the key players of a variety of paracrine and endocrine functions related to the lipid and glucose, and the regulation of the immune system [4], and stimulating, as a consequence, the development of new efficient methodologies for the preparation and analysis of BA analogs of bio-pharmacological interest [5–10].

In this framework, we recently reported a one-pot process for the production of highly pure glyco- and tauro-conjugated bile salts (BSS) using a continuous flow approach [11]. Advantages of our method compared to previous batch mode approaches

**Abbreviations:** BA, bile acid; BS, bile salt; UDCA, ursodeoxycholic acid; CDCA, chenodeoxycholic acid; DCA, deoxycholic acid; CA, cholic acid; HPLC, high-performance liquid chromatography; ELSD, evaporative light scattering detector; MS, mass spectrometry; DAD, diode array detector; LOD, limit of detection; LOQ, limit of quantification

\* Corresponding author: Tel.: +39 075 585 5131; fax: +39 075 585 5161.

E-mail address: natalini@chimfarm.unipg.it (B. Natalini).

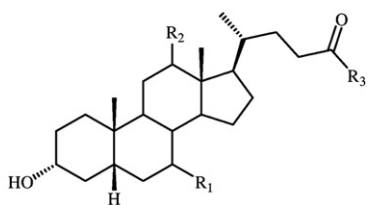
0039-9140/\$ - see front matter © 2012 Elsevier B.V. All rights reserved.

<http://dx.doi.org/10.1016/j.talanta.2012.07.092>

include the low cost and efficiency, the rapid optimization and precise control of the reaction conditions, the possibility to scale-up and continually process material on-demand with high yield and purity. The rapid and easy access to BA conjugates not only will help the candidate selection of BA analogs as therapeutic agents in the treatment of metabolic and liver diseases [5–8], but it will also fill the constant request of these compounds for the detection of inborn errors of BA synthesis and metabolism [12], for the spectrometric determination of plasma levels of BAs [13], as well as for the study of bacterial overgrowth in the gastrointestinal tract [14].

The employment of flow chemistry in the process optimization of the BA *N*-acyl amidation required the validation of an *in-line* HPLC method for the rapid and effective determination of the reaction yields as well as of the purity grade of the synthesized conjugates under different flow set-ups and experimental conditions. In this context, a unique HPLC method was successfully established and validated for ursodeoxycholic (UDCA), chenodeoxycholic (CDCA), deoxycholic (DCA), cholic (CA) acids and for the corresponding glyco- and tauro-conjugated forms (Fig. 1), which allowed a fast access to the knowledge of the quality of a given synthesis process.

Because of the shared absence of relevant chromophoric moieties in the sample structure, an evaporative light scattering detector (ELSD) was profitably utilized for the analysis of such steroidal species. Besides the repeatedly proven effectiveness of



Compound #	Label	Trivial name	R <sub>1</sub>	R <sub>2</sub>	R <sub>3</sub>
1	UDCA	Ursodeoxychoic acid	β-OH	H	OH
2	GUDCA	Glyoursodeoxychoic acid	β-OH	H	NHCH <sub>2</sub> CO <sub>2</sub> H
3	TUDCA	Tauroursodeoxychoic acid	β-OH	H	NH(CH <sub>2</sub> ) <sub>2</sub> SO <sub>3</sub> H
4	CDCA	Chenodeoxychoic acid	α-OH	H	OH
5	GCDCA	Glycochenodeoxychoic acid	α-OH	H	NHCH <sub>2</sub> CO <sub>2</sub> H
6	TCDC	Taurochenodeoxychoic acid	α-OH	H	NH(CH <sub>2</sub> ) <sub>2</sub> SO <sub>3</sub> H
7	DCA	Deoxychoic acid	H	α-OH	OH
8	GDCA	Glycodeoxychoic acid	H	α-OH	NHCH <sub>2</sub> CO <sub>2</sub> H
9	TDCA	Taurodeoxychoic acid	H	α-OH	NH(CH <sub>2</sub> ) <sub>2</sub> SO <sub>3</sub> H
10	CA	Cholic acid	α-OH	α-OH	OH
11	GCA	Glycocholic acid	α-OH	α-OH	NHCH <sub>2</sub> CO <sub>2</sub> H
12	TCA	Taurocholic acid	α-OH	α-OH	NH(CH <sub>2</sub> ) <sub>2</sub> SO <sub>3</sub> H

Fig. 1. Compounds investigated in this study.

ELSD for the analysis of BAs and their derivatives [15–27], the employment of this “mass-sensitive” device also meets an advantageous cost-benefit compromise which makes it particularly attractive over mass spectrometer (MS) and charged aerosol detectors [15,28]. A major downside of ELSD is that no spectral information can be acquired, thus unabling to identify a certain peak or perform peak purity analysis as with MS or diod array (DAD) detectors. However, when used for assisting synthesis procedures, peak identification with HPLC/ELSD systems can be made basing on the retention time and co-injection with standard solutions [28].

For each of the compounds investigated in this study (Fig. 1), all the runs were contemporarily carried out on the acidic free and the two relative conjugated species. Analogously with other studies on structurally related compounds [24,29,30], also for BAs a different ELSD response from the free and the corresponding conjugated variants was observed. As a consequence of this evidence, the build-up of separate calibration curves was strictly required. In all the cases, very good precision and accuracy (evaluated both in the short and long period) along with remarkably low LOD and LOQ values were obtained.

The present study represents the first example of fully validated RP-HPLC/ELSD methods to apply to the simultaneous analysis of the main unconjugated human BAs and their corresponding glyco- and tauro-conjugated metabolites.

### 1.1. HPLC/ELSD- and UPLC/ELSD-based applications to BA analysis

BAs and derivatives belong to a very heterogeneous class of compounds in terms of both hydrophobic/hydrophilic balance extent and UV sorption power [31]. Focusing on the latter and accounting for the scarce sensitivity mainly for compounds which are devoid of chromophoric moieties, UV detection of unlabeled species can be however engaged in the range of 200–210 nm for analyses on glyco- and tauro-conjugated species [15]. Conversely, as previously advanced, this comes to be completely ineffective for the unconjugated ones [15].

In the early 90's, Roda and co-workers [21] reported for the first time on the extraordinary advantages deriving from the

utilization of a HPLC/ELSD system for the simultaneous analysis of an intricate mixture of amidated and free BAs. The authors clearly emphasized on the remarkable gain concerning the limit of detection (which also resulted comparable for compounds belonging to the two subclasses) as well as the compatibility with gradient elution-mode analyses. This latter aspect is highly instrumental when assays on hydrophobically different analytes are planned. Although the noteworthy benefits, only a limited number of applications dealing with HPLC/ELSD analyses on BAs and their derivatives was reported in the following years, with respect to those based on MS detection. Some of the most relevant contributions are briefly summarized in the following discussion.

Very interestingly, Kakiyama and co-workers [15] described a direct and effective RP-HPLC/ELSD method for the separation and quantification of a series of 24-acyl glycoside BAs derivatives, which can be classified among the BAs metabolites. Besides the very low determined detection limits, the authors claimed on the possibility to simultaneously analyze physico-chemically diverse BAs through defined gradient elution runs.

Yan and co-workers [24] proposed a liquid chromatographic method for the simultaneous quantification of nine ingredients in 19 different *Qingkailing* injection samples. Coupling a DAD with an ELSD permitted the determination, among others, of three structurally different unconjugated BAs which through a synergic effect render this well-known composite formula of the traditional Chinese medicine successful in the clinical treatment of several pathologies such as hepatitis, encephalitis, cerebral thrombosis.

By means of a HPLC/ELSD apparatus, Hong and co-workers [17] efficiently monitorized the effect exerted by a soluble dietary fiber (HydroxyPropyl MethylCellulose, HPMC) on excreted lipid in feces. With the aim to control the incidence of diet on the lipid adsorption as well as the profile of the fecal components, the author claimed the established method highly suitable, inter alia, for routine screening of the two secondary fecal BAs, namely DCA and lithocholic acid (LCA). The very low limits of detection and the possibility to operate in a gradient elution-mode were specifically remarked by the authors.

For the first time in 2003 Criado and co-workers [18] proposed the direct and automated ELSD screening of 10 primary and secondary BAs, directly from lyophilized biological fluids (serum and urine). The chromatographic step was successfully accomplished by means of a RP-HPLC gradient elution analysis and the ELSD furnished very appreciable detection limits for all the distinguished steroidal compounds. Worth mentioning in this study is the set-up of a very intriguing FI/HPLC/ELSD integrated apparatus which proved to be helpful in speeding-up the diagnosis of hepatobiliary disease and other gastro-intestinal problems.

Valuable contributions in this field were also given by the Xiao group. Accordingly, the authors proposed an effective gradient RP-UPLC method for the simultaneous determination of four unconjugated and one conjugated BAs in *Calculus bovis* and its medicinal preparation [25]. The validated chromatographic method provided the efficient base-line separation of the above five species within a very short analysis time. Worth to be mentioned are also the particularly appreciable detection and quantitation limits obtained. A very efficient gradient RP-UPLC/ELSD was established and validated by the same group to fully resolve a more intricate mixture of seven components, encompassing five unconjugated and one conjugated BAs, contained in natural *Calculus bovis* and its substitutes or spurious breeds [26]. Very fruitfully, by applying the PCA statistical method, the authors fulfilled the scope to discriminate *Calculus bovis* samples and its substitutes or spurious breeds, thus contributing to

provide some references for the quality control of *Calculus bovis* and other Chinese medicinal products. More recently, the same authors successfully applied an efficient RP-UPLC/ELSD method to establish the fingerprints of artificial *Calculus bovis* extracts from different extraction solvents [27]. The anti-bacterial activity of these extracts on *Staphylococcus aureus* growth was studied through microcalorimetric analysis, revealing that sodium taurocholate (TCANa), CA and CDCA represent the major anti-bacterial components in artificial *Calculus bovis*.

The re-flourished interest towards the BAs as versatile signaling hormones endowed with diverse endocrine functions stimulated us in the development of reliable analytical protocols to apply in monitoring the synthesis of new BA-based receptor modulators [19]. On this basis, a HPLC/ELSD study was engaged with the aim to set-up suitable chromatographic conditions for the analysis of three different epimeric couples of 23-methyl-substituted unconjugated BAs. Accordingly, three different methods were successfully established and then validated, assuring appreciable levels of precision and accuracy along with low LOD and LOQ values. Moreover, with the aim to avail of a chromatographic parameter enabling fast and reliable information on the critical micellar concentration (CMC) of pharmaceutically relevant unconjugated BAs, we recently developed a gradient RP-HPLC/ELSD method [20]. The statistically relevant mathematical relationship obtained between spectrophotometric CMCs and “chromatographic hydrophobicity index (CHI)” values can be of aid to rationally direct the synthesis of new BAs, mainly during the early stages of the drug-discovery process.

## 2. Materials and methods

### 2.1. Chemicals

All the reagents used to build-up the calibration curves were of analytical grade. Acetonitrile (MeCN), Ammonium formate ( $\text{HCO}_2\text{NH}_4$ ), and formic acid ( $\text{HCO}_2\text{H}$ ) were purchased from Sigma–Aldrich (Milano, Italy). HPLC-grade water was obtained from a tandem Milli-Ro/Milli-Q apparatus (Millipore, Bedford, MA, USA). Standard free and conjugated bile acids were kindly provided by Erregierre (Bergamo, Italy).

### 2.2. Instrumentation

The analytical HPLC measurements were made on a Shimadzu (Kyoto, Japan) LC-20A Prominence equipped with a CBM-20A communication bus module, two LC-20AD dual piston pumps, and a Rheodyne 7725i injector (Rheodyne Inc., Cotati, CA, USA) with a 20  $\mu\text{L}$  stainless steel loop.

A Varian 385-LC evaporative light scattering detector (ELSD) (Agilent Technologies, Santa Clara, CA, USA) was utilized for the analyses. The analog-to-digital conversion of the output signal from the ELSD was allowed by a common interface device. The adopted ELSD conditions for the analysis of all BAs were: 30 °C nebulization temperature, 50 °C evaporation temperature, 1.5 L  $\text{min}^{-1}$  gas flow rate (air) and 2.0 as the gain factor.

A GraceSmart RP18 column (Grace, Sedriano, Italy) 250  $\times$  4.6 mm i.d., 5  $\mu\text{m}$ , 100 Å was used as the analytical column. The column temperature was controlled through a Grace (Sedriano, Italy) heater/chiller (Model 7956R) thermostat.

### 2.3. RP-HPLC isocratic analysis

The mobile phase was prepared by dissolving  $\text{HCO}_2\text{NH}_4$  in a  $\text{H}_2\text{O}/\text{MeCN}$ —60/40 (v/v) solution so as to get a 50 mM buffer concentration; then, the apparent pH [ $^{\text{s}}\text{pH}$ , that is the one

measured in the employed hydro-organic mobile phase (s), while the calibration of the pH system was done in water (w)] was adjusted to 3.5 with  $\text{HCO}_2\text{H}$ . The analyses were carried out at a 1.0  $\text{mL min}^{-1}$  eluent flow rate after previous conditioning by passing through the column the selected mobile phase for at least 30 min at the same eluent velocity. Before being used, all the mobile phases were always filtered through a 0.22  $\mu\text{m}$  Millipore filter (Bedford, MA, USA) and then degassed with 20 min sonication. All the analyses were conducted at a 25 °C column temperature.

### 2.4. Selected chromatographic parameters

All the following chromatographic parameters were calculated according to the German Pharmacopeia (DAB). The retention factor ( $k$ ) values were computed by taking the retention time ( $t_R$ ) at the peak maximum. Separation factor ( $\alpha$ ) and resolution factor ( $R_S$ ) values were computed from the following Eqs. (1) and (2):

$$\alpha = \frac{k_2}{k_1} \quad (1)$$

$$R_S = 1.18 \frac{t_R - t_{Rp}}{W_{0.5} + Wp_{0.5}} \quad (2)$$

where  $k_1$  is the retention factor of the first eluted compound for each of the considered couples,  $k_2$  is the retention factor of the second eluted compound for each of the considered couples,  $W_{0.5}$  is the width of the peak at the position of 50% peak height,  $Wp_{0.5}$  is the width of the peak at the position of previous 50% peak height and  $t_{Rp}$  is the retention time of the first eluted peak within each considered couple.

## 3. Results and discussion

By taking into account the different lipophilicity and  $pK_a$  value between the free and the corresponding amidated BAs [31], the preliminary identification of a unique mobile phase composition enabling the separate isocratic resolution of each of the four triplets of compounds was thought to be an essential step for a rapid evaluation of all the experienced synthetic procedures. Therefore, with the aid of opportunely prepared sample mixtures, containing the free BA and the corresponding glyco- and tauro-derivative, a suitable eluent composition was established (see Experimental part for details), which allowed in all the cases the peak resolution within usable retention times (Table 1). With the

**Table 1**  
Selected chromatographic data (retention factor  $k$ , separation factor  $\alpha$ , and resolution factor  $R_S$  values) obtained in the analysis of the investigated compounds 1–12.

Compound #	Selected chromatographic parameters		
	$k$	$\alpha$	$R_S$
1	0.79		
2	2.18	2.76	16.77
3	6.50	2.98	33.07
4	1.86		
5	5.19	2.79	24.54
6	15.97	3.08	37.18
7	2.22		
8	5.96	2.68	24.93
9	17.49	2.93	35.23
10	0.72		
11	1.78	2.47	12.09
12	4.69	2.63	22.22

selected eluent mixture, the following elution order turned out for all triplets of compounds: tauro-conjugated derivative < glyco-conjugated derivative < free form. Due to the eluent conditions, all compounds were predominantly present in their acidic form during HPLC analysis.

Moreover, being aware that the gas flow rate along with the nebulization and the evaporation temperatures markedly affect the response efficiency of ELSD [22,32], preliminary efforts were also addressed to establish the best detection set-up compromise for all the investigated compounds (see Experimental part for details). To rely upon the air as the gas carrier instead of the more common nitrogen [19,20,33] was dictated by practical and economical reasons. In comparison with other applications with similar eluent systems [24,34], running the analyses at a lower evaporation temperature (50 °C) was made possible by the nebulization temperature being tuneable.

More in depth, as a result of the technological peculiarity of the employed ELSD, a more fruitful control of the atomization process (that is the droplet dimension) and, in turn, of the following solvent evaporation step [19,20] is allowed.

Since ELSD does not provide any structural information, for all compounds the peak identification was based on retention time and co-injection with standard solutions.

### 3.1. Method validation

#### 3.1.1. Selectivity

Aimed at identifying the presence of interference peaks within the investigated analysis time, three chromatograms of the selected solvent blank (namely the eluent system) were consecutively run. The peaks obtained (with very small areas in arbitrary units) did not overlap those corresponding to the submitted 12 compounds.

Moreover, very appreciable separation ( $\alpha$ ) and resolution factor ( $R_s$ ) values between the peaks from each of the four submitted triplets of samples (Table 1) were achieved with the selected eluent system.

On this basis, the established method can be regarded as highly selective for the purpose of the present study.

#### 3.1.2. Linearity

With the same modus operandi, independent sets of analyses were performed on the 12 compounds. In all the cases, five calibration standards having concentration values uniformly spanning within the ranges specified in Table 2 were used.

For each BA, the concentration range of the corresponding linearity curve was adapted to the compound concentration as provided by the flow reactor output after acidification. More in

depth, the extreme concentration values of each range were established as the ones approximately producing a 5 to 15 folds lower and higher peak area value than that generated by the compound solution. The direct analysis of the sample solution was deemed to be of essential importance to speed-up as much as possible the control of a given synthetic process. Moreover, it should be stated that to consider wide concentration ranges for the unconjugated free forms was not strictly required due to their nature as impurity in each synthetic procedure.

In contrast to conventional UV detectors where a linear correlation between the peak area response ( $A$ ) and the analyte mass ( $m$ ) occurs, the relationship between the output signal and the amount of mass present in an ELSD device is of a non-linear nature [28,32,35]. Indeed, peak area values are correlated to the corresponding analyte mass (or concentration) quantities by the well-established exponential curve as follow Eq. (3):

$$A = am^b \quad (3)$$

where the value of the  $a$  and  $b$  coefficients strictly depends on both the sample nature and the selected analysis conditions.

The exponential profile of the peak area vs analyte concentration plots is exemplarily shown in Fig. 2a for UDCA (1) and the corresponding glyco (2)- and tauro (3)-conjugated forms and in Fig. 2b for CA (10) and the corresponding glyco (11) and tauro (12)-conjugated.

After the log–log transformation of Eq. (3) being carried out [28,32,35], thus affording the general Eq. (4)

$$\log A = b \log m + \log a \quad (4)$$

linear curves were obtained ( $R^2$  values within the range 0.989–0.999) (Table 2), and then profitably used for the method validation study. All the calibration standards were analyzed in triplicate and the average value of the corresponding peak area utilized to build-up the regression line.

As far as the equations in Table 2 are concerned, while  $y$  represents the log value of the peak area,  $x$  corresponds to the log transformation of the sample concentration value. Evidently, even subtle variations in the analyte structure (Fig. 1) can generate different calibration curves, which is in line with the observation reported by other authors [24,29,30]. Inherently, more relevant differences were found between the unconjugated species and the corresponding conjugated variants (Table 2).

With the aid of equally concentrated solutions of 1, 2 and 3 (Fig. 3a), and 10, 11 and 12 (Fig. 3b), the dissimilar ELSD signal output at the fixed analysis conditions is exemplarily shown, which is consistent with the slope value ranking of the relative regression equation in Table 2.

**Table 2**

Calibration data for compounds 1–12: regression equations, correlation coefficient ( $R^2$ ) values, explored linearity ranges, LOD and LOQ values.

Compound #	Regression equation	$R^2$	Linearity range ( $\mu\text{g mL}^{-1}$ )	LOD ( $\text{ng mL}^{-1}$ )	LOQ ( $\text{ng mL}^{-1}$ )
1	$y = 2.25 (\pm 0.03)x + 2.56 (\pm 0.04)$	0.997	10–60	27	44
2	$y = 1.66 (\pm 0.01)x + 2.58 (\pm 0.03)$	0.999	40–240	5	9
3	$y = 1.71 (\pm 0.02)x + 2.47 (\pm 0.04)$	0.998	40–240	7	14
4	$y = 1.40 (\pm 0.02)x + 3.16 (\pm 0.05)$	0.996	40–240	1	2
5	$y = 1.77 (\pm 0.01)x + 2.15 (\pm 0.02)$	0.999	40–240	9	17
6	$y = 1.56 (\pm 0.04)x + 2.77 (\pm 0.08)$	0.992	40–240	5	9
7	$y = 1.39 (\pm 0.04)x + 3.00 (\pm 0.08)$	0.989	40–240	2	4
8	$y = 1.77 (\pm 0.01)x + 2.31 (\pm 0.02)$	0.999	60–320	7	14
9	$y = 1.67 (\pm 0.01)x + 2.68 (\pm 0.02)$	0.999	40–240	3	6
10	$y = 1.45 (\pm 0.03)x + 2.98 (\pm 0.05)$	0.993	8–60	2	5
11	$y = 1.73 (\pm 0.02)x + 2.63 (\pm 0.03)$	0.999	20–120	6	12
12	$y = 1.73 (\pm 0.01)x + 2.66 (\pm 0.02)$	0.999	20–120	4	8

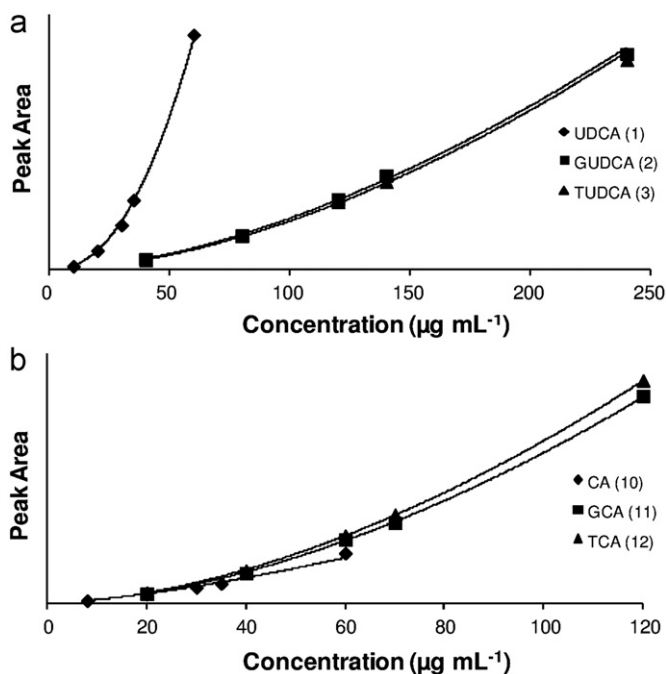


Fig. 2. Linear calibration curves obtained for (a) UDCA (1) and its glyco (2) and tauro (3) conjugates and (b) CA (10) and its glyco (11) and tauro conjugates.

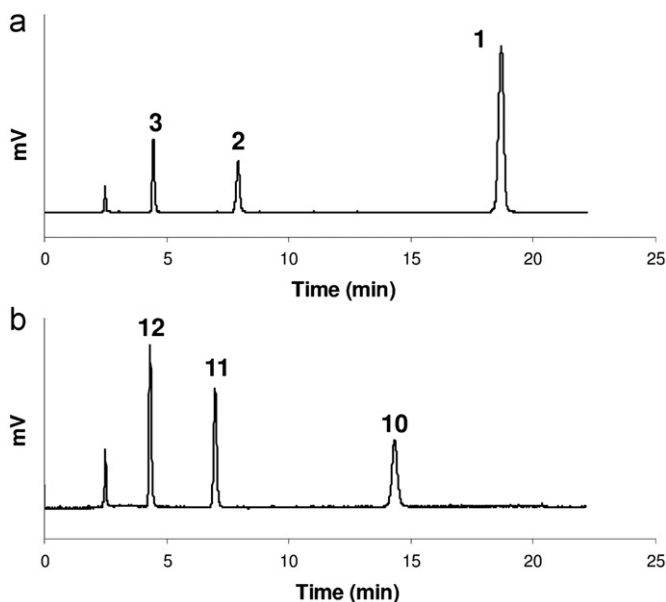


Fig. 3. Chromatographic trace obtained with solutions of (a) equally concentrated UDCA (1) and its glyco (2) and tauro (3) conjugates and (b) equally concentrated CA (10) and its glyco (11) and tauro (12) conjugates.

### 3.1.3. LOD and LOQ

By utilizing the mathematical models (regression equations) reported in Table 2, very appreciable LOD and LOQ values (the former being within the range 1–27 ng mL<sup>-1</sup> and the latter within the range 2–44 ng mL<sup>-1</sup>, Table 2) were determined.

Interestingly, despite their very similar regression equations (Table 2), different LOD and LOQ values were instead computed for GCA (11) and TCA (12). This finding is explained by the different value of the standard error ( $\sigma_y$ ) of the corresponding regression (0.02 and 0.01 for 11 and 12, respectively), which is

included in the following Eqs. (5) and (6)

$$C_{LOD} = 3.3 \frac{\sigma_y}{b} \quad (5)$$

$$C_{LOQ} = 10 \frac{\sigma_y}{b} \quad (6)$$

where  $C_{LOD}$  and  $C_{LOQ}$  are the sample concentrations corresponding to the LOD and LOQ, respectively, and  $b$  is the slope of the relative calibration equation (Table 2).

### 3.1.4. Intra-day and inter-day precision

Intra-day precision was assessed for each of the twelve investigated compounds by using of the appropriate calibration curve as formalized by the equations listed in Table 2. For all compounds, an external set of two control solutions with concentration as indicated in Table 3 was run in triplicate ( $n=3$ ) within a period of approximately 2–4 h, depending on the retention time of the specific BA to be analyzed. The procedure was repeated for a period of three consecutive days. The previously obtained mathematical models (Table 2) were then used to calculate the concentrations of the control solutions (mean observed concentrations, Table 3).

The intra-day precision was evaluated as the relative standard deviation (RSD%) among the concentration values achieved from consecutive injections. For each control solution, the variation within replicate injections performed during a three consecutive day period (and hence a total of nine injections,  $n=9$ ) was used to calculate the inter-day precision.

As shown in Table 3, a comparable and very appreciable range of variation in the RSD% values was observed during the consecutive three days of analysis: 0.27–4.00% for day 1, 0.27–5.15% for day 2, and 0.35–5.22% for day 3. This, in turn, clearly indicates a highly reproducible detector response, which ensures a profitable stability of the HPLC/ELSD method under validation.

In accordance with the estimated intra-day precision results, satisfactory RSD% values (ranging from 1.04 to 6.40%) were also recorded when the long term (inter-day) precision was evaluated (Table 4).

In Fig. 4a, the average RSD% value of the long-term period is reported for each compound. Clearly, for 4 and 7 the method resulted less precise than the overall average precision (corresponding the RSD% to 3.20 and evidenced by the dotted line). By contrast, the method was found on the average more precise for 9 and 12.

### 3.1.5. Intra-day and inter-day accuracy

The “Recovery test” approach (percentage recovery) [28] was selected to estimate the accuracy of the established HPLC/ELSD method. For each determination, the value was calculated according to the following formula Eq. (7)

$$\text{Recovery}\% = \frac{C_{\text{measured}}}{C_{\text{theoretical}}} 100 \quad (7)$$

where  $C_{\text{measured}}$  represents the sample concentration as calculated through the regression equation in Table 3 (mean observed concentration), while  $C_{\text{theoretical}}$  corresponds to the concentration of the employed external test solution (theoretical concentration).

By analogy with the estimation of short and long term precision, intra-day and inter-day accuracy were also calculated with the same external solutions (Table 3). Accordingly, while the former was determined by taking into account the three runs for each control solution within a single day ( $n=3$ ), for the latter, the average value from nine ( $n=9$ ) determinations (during the three days of analysis) was considered.

While the percentage recovery lay between 90.87 and 107.37% during the first day of analysis (day 1, Table 3), the value varied

**Table 3**  
Statistical analysis for compounds **1–12** in the short period (intra-day precision and accuracy values).

Compound #	Solution	Theoretical concentration ( $\mu\text{g mL}^{-1}$ )	Day	Mean observed concentration ( $\mu\text{g mL}^{-1}$ )	$n^a$	Precision (RSD%)	Accuracy (Recovery%)
<b>1</b>	1	15	1	14.87	3	2.35	99.16
			2	14.72		0.48	98.15
			3	16.22		2.53	108.06
	2	40	1	40.71	3	1.18	101.78
			2	39.22		1.22	98.03
			3	42.14		1.78	105.35
<b>2</b>	1	60	1	54.52	3	4.00	90.87
			2	59.76		2.44	99.60
			3	59.07		1.03	98.45
	2	160	1	158.49	3	0.83	99.06
			2	158.87		1.82	99.30
			3	158.74		1.16	99.21
<b>3</b>	1	60	1	63.63	3	0.27	106.05
			2	61.04		1.16	101.67
			3	59.64		2.98	99.38
	2	160	1	169.59	3	0.53	105.98
			2	158.21		0.83	98.83
			3	161.97		0.35	101.21
<b>4</b>	1	60	1	59.96	3	1.05	99.97
			2	64.04		1.58	106.71
			3	64.58		0.74	107.69
	2	160	1	161.85	3	0.81	101.21
			2	166.09		1.46	103.81
			3	185.52		1.05	115.85
<b>5</b>	1	60	1	61.31	3	2.76	102.24
			2	61.54		5.15	102.54
			3	65.05		1.31	108.45
	2	160	1	159.61	3	2.93	99.85
			2	161.27		1.39	100.83
			3	168.86		1.92	105.58
<b>6</b>	1	60	1	57.02	3	1.16	95.11
			2	59.22		2.86	98.62
			3	62.63		1.61	104.37
	2	160	1	171.71	3	1.19	107.37
			2	178.98		2.78	111.94
			3	182.56		1.75	114.12
<b>7</b>	1	60	1	60.05	3	2.51	100.14
			2	58.74		3.92	97.89
			3	54.04		0.70	90.06
	2	160	1	155.16	3	2.62	97.05
			2	163.33		2.91	102.02
			3	164.52		3.24	102.89
<b>8</b>	1	80	1	81.48	3	2.63	101.71
			2	79.58		3.24	99.4
			3	81.17		5.22	101.39
	2	240	1	239.44	3	1.39	99.65
			2	240.47		0.93	100.11
			3	241.16		1.61	100.48
<b>9</b>	1	60	1	58.85	3	1.95	98.07
			2	57.95		3.17	98.68
			3	58.64		2.32	97.78
	2	160	1	161.70	3	1.41	101.21
			2	162.71		1.16	101.76
			3	164.67		1.30	104.00
<b>10</b>	1	14	1	14.12	3	1.84	100.83
			2	13.99		2.65	99.91
			3	14.56		2.43	103.97
	2	40	1	39.42	3	2.69	98.56
			2	40.01		0.40	99.99
			3	41.37		0.75	103.34
<b>11</b>	1	30	1	29.58	3	2.91	98.63
			2	30.47		4.24	101.5
			3	30.74		1.53	102.47
	2	80	1	81.13	3	1.08	101.45
			2	83.19		1.06	103.97
			3	84.23		0.94	105.26
<b>12</b>	1	30	1	29.58	3	0.91	98.60
			2	29.76		0.34	99.13
			3	30.12		0.83	100.44
	2	80	1	78.38	3	1.00	97.93
			2	81.73		0.27	102.15
			3	81.69		1.06	102.23

<sup>a</sup> Number of replicates.

**Table 4**  
Statistical analysis for compounds 1–12 in the long period (inter-day precision and accuracy values).

Compound #	Solution	Theoretical concentration ( $\mu\text{g mL}^{-1}$ )	Mean observed concentration ( $\mu\text{g mL}^{-1}$ )	$n^a$	Precision (RSD%)	Accuracy (Recovery%)
1	1	15	15.27	9	4.98	101.79
	2	40	40.69		3.37	101.72
2	1	60	57.76	9	4.86	96.31
	2	160	158.69		1.16	99.19
3	1	60	61.44	9	3.27	102.37
	2	160	163.26		3.13	102.00
4	1	60	62.86	9	3.63	104.79
	2	160	171.16		6.4	106.96
5	1	60	62.63	9	4.13	104.41
	2	160	163.25		3.21	102.09
6	1	60	59.63	9	4.43	99.36
	2	160	177.75		3.20	111.14
7	1	60	57.61	9	5.35	96.03
	2	160	161.00		3.73	100.65
8	1	80	80.74	9	3.51	100.83
	2	240	240.36		1.21	100.06
9	1	60	58.48	9	2.29	97.51
	2	160	163.03		1.39	101.02
10	1	14	14.05	9	2.74	101.58
	2	40	40.27		2.52	100.63
11	1	30	30.26	9	3.17	100.87
	2	80	82.85		1.85	103.56
12	1	30	29.82	9	1.04	99.39
	2	80	80.60		2.25	100.77

<sup>a</sup> Number of replicates.

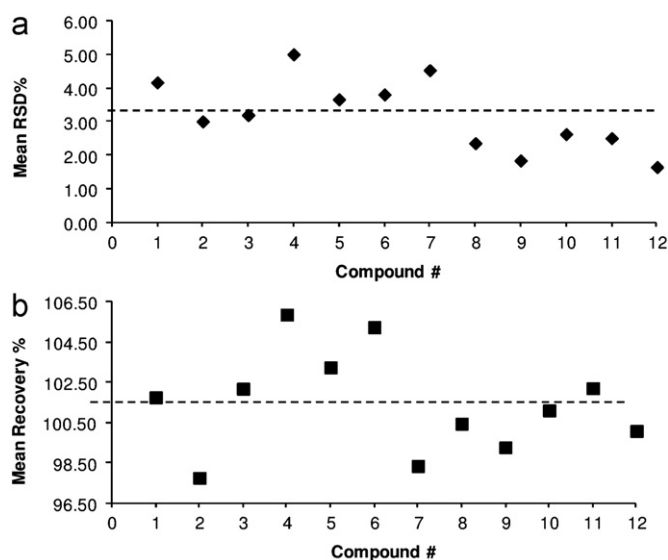


**Fig. 4.** Average (a) RSD% and (b) Recovery% values of compounds 1–12, determined in the long period. Dotted lines indicate the corresponding overall average value.

within a narrower range during day 2, being it included in between 97.89 and 111.94%. The broadest interval of variation occurred during day 3: 90.06–115.85% (Table 3).

A good accuracy was also computed in the long term (inter-day) period, spanning the Recovery% in the range 96.03–111.14% (Table 4).

In the long period, the overall average Recovery% was calculated as equal to 101.46 (Fig. 4b). Moreover, the developed HPLC/ELSD method was found on the average to be less accurate for 2, 4, 6 and 7, with respect to the other compounds.

#### 4. Conclusions

As a continuing interest in BAs field, we have reported a validated HPLC/ELSD method for a rapid *in-line* screening of diverse synthetic procedures, thus contributing to identify optimal experimental conditions for the synthesis of amidated BA derivatives by using a continuous flow approach. On the basis of the high quality of the validated method (RSD % and Recovery% in the long period spanning, respectively, in the range 1.04%–6.40% and 96.03%–111.14%; LOD and LOQ values within the range 1–27  $\text{ng mL}^{-1}$  and 2–44  $\text{ng mL}^{-1}$ , respectively), along with the recognized advantages of ELSD over other types of detectors, analog analytical approaches will be electively pursued for future flow synthesis-based production of BA derivatives of biological interest.

#### References

- [1] R. Sharma, A. Long, J.F. Gilmer, *Curr. Med. Chem.* 18 (2011) 4029–4052.
- [2] A.F. Hofmann, L.R. Hagey, *Cell. Mol. Life Sci.* 65 (2008) 2461–2483.
- [3] P. Lefebvre, B. Cariou, F. Lien, F. Kuipers, B. Staels, *Physiol. Rev.* 89 (2009) 147–191.
- [4] C. Thomas, R. Pellicciari, M. Pruzanski, J. Auwerx, K. Schoonjans, *Nat. Rev. Drug Discov.* 7 (2008) 1–18.
- [5] R. Pellicciari, A. Gioiello, P. Sabbatini, F. Venturoni, R. Nuti, C. Colliva, G. Rizzo, L. Adorini, M. Pruzanski, A. Roda, A. Macchiarulo, *ACS Med. Chem. Lett.* 3 (2012) 273–277.
- [6] A. Gioiello, A. Macchiarulo, A. Carotti, P. Filippini, G. Costantino, G. Rizzo, L. Adorini, R. Pellicciari, *Bioorg. Med. Chem.* 19 (2011) 2650–2658.
- [7] Y. Iguchi, M. Yamaguchi, H. Sato, K. Kihira, T. Nishimaki-Mogami, M. Une, *J. Lipid Res.* 51 (2010) 1432–1441.
- [8] R. Pellicciari, A. Gioiello, A. Macchiarulo, C. Thomas, E. Rosatelli, B. Natalini, R. Sardella, M. Pruzanski, A. Roda, E. Pastorini, K. Schoonjans, J. Auwerx, *J. Med. Chem.* 52 (2009) 7958–7961.
- [9] H. Sato, A. Macchiarulo, C. Thomas, A. Gioiello, M. Une, A. Hofmann, R. Saladin, K. Schoonjans, R. Pellicciari, J. Auwerx, *J. Med. Chem.* 51 (2008) 1831–1841.

- [10] R. Pellicciari, G. Costantino, E. Camaioni, B.M. Sadeghpour, A. Entrena, T.M. Willson, S. Fiorucci, C. Clerici, A. Gioiello, *J. Med. Chem.* 47 (2004) 4559–4569.
- [11] F. Venturoni, A. Gioiello, R. Sardella, B. Natalini, R. Pellicciari, *Org. Biomol. Chem.* 10 (2012) 4109–4115.
- [12] E.J. Heubi, K.D.R. Setchell, K.E. Bove, *Semin. Liver Dis.* 27 (2007) 282–294.
- [13] A. Roda, F. Piazza, M. Baraldini, *J. Chromatogr. B* 717 (1998) 263–278.
- [14] J.R. Mathias, M.H. Clench, *Am. J. Med. Sci.* 289 (1985) 243–248.
- [15] G. Kakiyama, A. Hosoda, Y. Fujimoto, T. Goto, N. Mano, J. Goto, T. Nambara, *J. Chromatogr. A* 1125 (2006) 112–116.
- [16] E.C. Torchia, E.D. Labonté, L.B. Agellon, *Anal. Biochem.* 298 (2001) 293–298.
- [17] Y.J. Hong, M. Turowski, J.T. Lin, W.H. Yokoyama, *J. Agric. Food Chem.* 55 (2007) 9750–9757.
- [18] A. Criado, S. Cárdenas, M. Gallego, M. Valcárcel, *J. Chromatogr. B* 792 (2003) 299–305.
- [19] B. Natalini, R. Sardella, A. Gioiello, G. Carbone, M. Dawgul, R. Pellicciari, *J. Sep. Sci.* 32 (2009) 2022–2033.
- [20] B. Natalini, R. Sardella, A. Gioiello, E. Rosatelli, F. Ianni, E. Camaioni, R. Pellicciari, *Anal. Bioanal. Chem.* 401 (2011) 267–274.
- [21] A. Roda, C. Cerrè, P. Simoni, C. Polimeri, C. Vaccari, A. Pistillo, *J. Lipid Res.* 33 (1992) 1393–1401.
- [22] R. Lucena, S. Cárdenas, M. Valcárcel, *Anal. Bioanal. Chem.* 388 (2007) 1663–1672.
- [23] K. He, G.F. Pauli, B. Zheng, W. Huikang, B. Naisheng, T. Peng, M. Roller, Q. Zheng, *J. Chromatogr. A* 1112 (2006) 241–254.
- [24] S. Yan, G. Luo, Y. Wang, Y. Cheng, *J. Pharm. Bioanal. Chem.* 40 (2006) 889–895.
- [25] W. Kong, C. Jin, W. Liu, X. Xiao, Y. Zhao, Z. Li, P. Zhang, X. Li, *Food Chem.* 120 (2010) 1193–1200.
- [26] W. Kong, C. Jin, X. Xiao, Y. Zhao, W. Liu, Z. Li, P. Zhang, *J. Sep. Sci.* 33 (2010) 1518–1527.
- [27] Q. Zang, J. Wang, W. Kong, C. Jin, Z. Ma, J. Chen, Q. Gong, X. Xiao, *J. Sep. Sci.* 34 (2011) 3330–3338.
- [28] N. Vervoort, D. Daemen, G. Török, *J. Chromatogr. A* 1189 (2008) 92–100.
- [29] A. Müller, M. Ganzer, H. Stuppner, *J. Chromatogr. A* 1112 (2006) 218–223.
- [30] M.J. Dubber, I. Kanfer, *J. Chromatogr. A* 41 (2006) 135–140.
- [31] K.D.R. Setchell, D. Kritchevsky, P.P. Nair, *The Bile Acids: Chemistry, Physiology, Metabolism*, fourth ed., Springer Verlag GmbH, New York, 1988.
- [32] M. Kohler, W. Haerdi, P. Christen, J.L. Veuthey, *Trends Anal. Chem.* 16 (1997) 475–484.
- [33] I. Clarot, P. Chaimbault, F. Hasdenteufel, P. Netter, A. Nicolas, *J. Chromatogr. A* 1031 (2004) 281–287.
- [34] C.Z. Liu, H.Y. Zhou, Y. Zhao, *Anal. Chim. Acta* 581 (2007) 298–302.
- [35] E.G. Galanakis, N.C. Megoulas, P. Solich, M. Koupparis, *J. Pharm. Bioanal. Chem.* 40 (2006) 1114–1120.